IJISET - International Journal of Innovative Science, Engineering & Technology, Vol. 4 Issue 2, February 2017
ISSN (Online) 2348 – 7968 | Impact Factor (2016) – 5.264
www.ijiset.com

Assessment Of Ground Penetrating Radar To Map The Archaeological Ruins In Valley Of The Golden Mummies (Vgm), Bahariya Oasis, Western Desert, Egypt

Abd El-Hafeez Th. H.[1], Magdey A. Attya[2] , El-Sayed A. Issawy[2], Ali F. Mohammed[1] and M. Rashwan[2]

1) Geology Department, Faculty of Science, Al-Azhar University, Egypt.
2) National Research Institute of Astronomy and Geopyhsics, Helwan.

Abstract

The Valley of the Golden Mummies, here referred to as VGM, is an impressive unique archaeological phenomena, not only for Egypt, but worldwide. It is located about 380 km west of Giza pyramids. The site was discovered around the last decade of the past century by Egyptian inspectors.

In 1999, the Supreme Council of Antiquities “SCA" composed a high stated and professional team of archaeologists, conservators, restorers, an epigrapher, architect, and a draftswoman. This started a significant and careful excavation at VGM. Within few weeks, the mission cleared four tombs with105 mummies that mostly cased in gold, in addition to many bracelets, necklaces, earrings, wine jars and coins. The coins were found placed in the hand of the deceased thought to have been designated for use as payment in the afterlife. The date of remains back to Roman Period mummies ever found in Egypt. These remains are around 2000 years old, but they are in remarkable condition.

In 2012, the National Research Institute of Astronomy and Geophysics "NRIAG" launched the STDF project "ID: 4168" to lineout the boarders of VGM and construct a map for the inside ruins, the present paper introduces particular results of the project.

Since the site is tentatively allocated and has no accurate maps, the working team established three geodetic reference points, outside the valley, used to correct location of the surveys inside and around the valley. Then, the

valley was divided in measuring cells, 50m by 50m, with accurate coordinates and labeled corners. GPR survey was conducted using the SIR-2000 attached to a 400 MHz antenna at cells XXX, with total area of 150 m×300 m. Grid pattern survey in zig-zag pattern with profile interval 1-2 m. the acquired data was processed using Reflexw Version 7.0 software. The interpretation outcome produces several 2D GPR records and time slices with high precision allocation. The results showed the existence of several buried tombs and features at different burial levels.

Keywords: VGM, GPR, Time slices, 3D Cub.

Introduction

Ground Penetrating Radar "GPR" is commonly used for archaeological investigations. The technique is very time effective and cost saver, i.e., it helps to reveal wide areas in short times and low cost. GPR is the only near surface geophysical tool that can make 3D maps and images of the subsurface at archaeological sites. GPR technique involves transmitting radar waves from a surface antenna, reflecting them off buried discontinuities and measuring the elapsed time before the reflections are received again at the surface (Davis and Annan, 1989).

One of the first applications to archaeology was conducted at Chaco Canyon, New Mexico (Vickers and Dolphin, 1975). These studies followed by a number of GPR applications in archaeology (Fischer et al., 1980; Sheets et al., 1985; Imai et al., 1987; Goodman, 1994; Goodman and Nishimura, 1993; Goodman et al., 1994; Goodman et al., 1995; Conyers, 2004; Conyers and Goodman, 1997 and Goodman et al., 1998). The development of the amplitude slice maps and computer programs made GPR technology more understandable to the archaeological community and able to produce synthetic computer models

of buried archaeological features and associated stratigraphy, which were also used as an aid in interpretation during data analysis (Conyers, 1995; Goodman 1994). In Egypt GPR is successfully used in imaging the subsurface at several archeological sites (Khozym, 2003 and 2007; Abbas et al., 2005; Mahfooz et al., 2008; Sayed, 2012 and Magdy et al., 2008 and 2012).

The Valley of the Golden Mummies "VGM" is a unique archaeological phenomina at Bahriya Oasis (Fig. 1), about 380 km west of the Giza pyramids. The valley is passing critical situation due to the allocation, the outlining, and the storing conditions; therefore, in 2012, NRIAG launched STDF ID: 4168 project to overcome these problems.

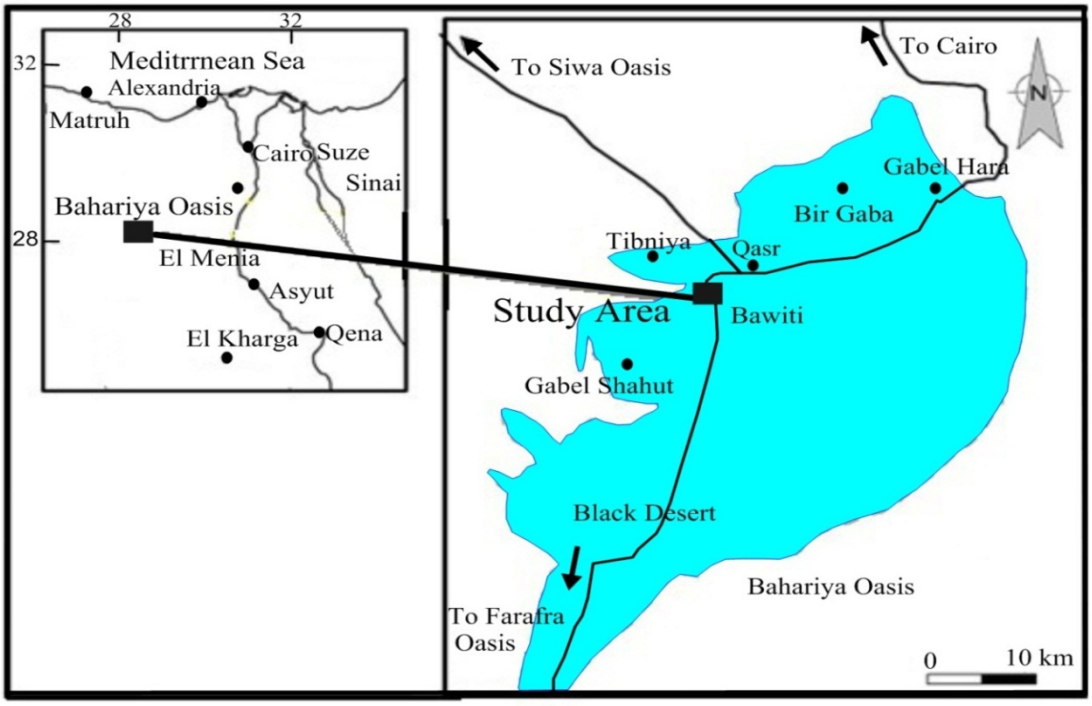

Fig. : 1 Location map of the study area

GPR survey was conducted using SIR 2000 with the 400 MHz, zig-zag configuration was used to acquire 3D grids at cells XXX. The outcome is a series of 2D section and slice maps for different depths. Several signatures for tombs and artifacts could be identified.

Point and Solution's vision

VGM accurate map and the inner artifact's content are not known so that, the neighbors cutting areas from the valley and add them to their farms. Also, people cross the valley with their cars and animals. Therefore, a geophysical program was conducted to achieve the following goals:

1. Allocate the outer boarders of the valley.
2. Define save roads network inside the valley.
3. Map and document the archaeological ruins in the valley.

This program was funded through the Science and Technology Developing Fund "STDF" ID: 4168. In this paper, we show some results of this project.

Site Description

The study area is close to be flat. The top soil is composed of coarse to fine ferruginous sandstone, the area is a part of the largest combinations of the Greco-Roman antiquities that considered as one of the most significant archaeological discoveries in the history of Egypt and the world. It contains many mummies cased in gold and some of them exposed on the surface (Fig.2).

Fig. : 2 A shows The discovered mummies B shows the complete ancient mummies which exposed on the surface.

Data Acquisition

Within this part, we concern acquiring three types of data; Allocating and Land Marking Constructing GPS reference points. The working team selected three locations adequate for constructing the GPS base stations according to the international standards. Due to the soft nature of the soil, we had to invade a steel net into the ground for more than one meter leaving 25cm over the ground surface. Then we fixed the planted portion of the steel net with concrete to assure the stability of the base station, also we cased the upper surface portion with concrete to avoid erosion (Fig. 3). This foundation has been leveled with cupper tipper. A GPS antenna is installed on the cupper tipper and conducted with GPS devices, the three base stations have been left acquiring coordinates for 8 hours recording 120 reading per hour to optimize the coordinate's precision.

Fig. 3: Construction and Installations of GPS Base Stations

Land Marking

The only known landmark at the site was a tomb excavated by the SCA team in 1999. We considered a side of this tomb as our start point and corrected its coordinates to the base stations, and labeled it as A_0. From this point out, we expand dividing the site into 50m by 50m cells (Fig. 4), the four corners of each cell are marked and their coordinates were corrected to the base stations. The labels are chained as A_0, A_1 … and B_0, B_1…etc. we kept the directions of the

cells' boards fit or close to the original geographic directions. These cells were used as the basic survey grid for the geophysical data acquiring.

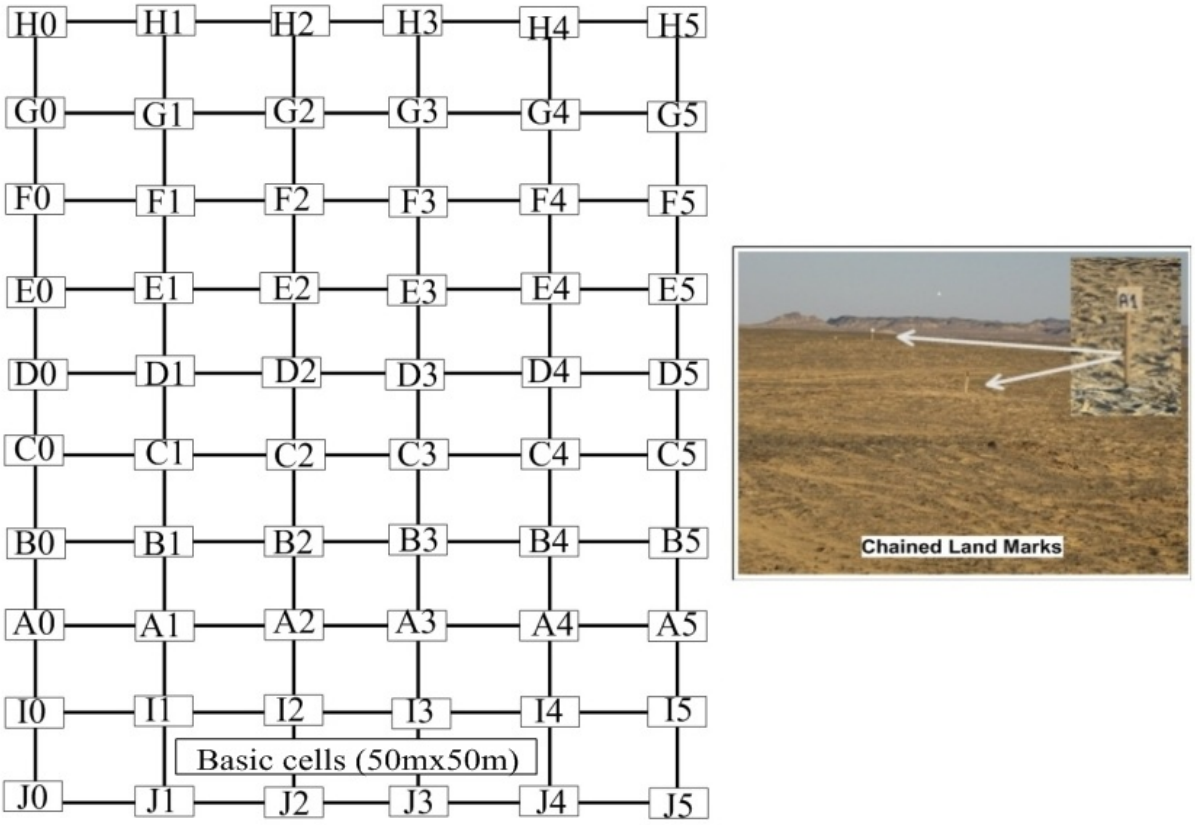

Fig. 4: Allocating and land marking the measuring cells.

1. Geodetic Survey.

Since the used antenna is 400MHz antenna, i.e. low depth penetration, it was necessary to survey the topographic elevation for the area of interest. After computing the corrected reference stations, we have used them every time we have observed these bases using the kinematic mode (Stop and Go technique). Then we used the GPS 4000 SSI model to observe the geodetic elevation at the area. The topographic data has been collected with a very high accuracy reaching to less than one centimeter. The collected data is processed using the GPS Processing Program Trimble Business Center (TBC) to get the coordinates of this area, these coordinates are referenced to the Ellipsoid, the projection used was UTM (Universal Transverse Mercator) Zone 36N, the Datum is WGS 84 (World Geodetic System 1984), and the

Geoidal Model is EGM96 (Earth Geoidal Model 1996). The resulting topographic map is given in figure 5.

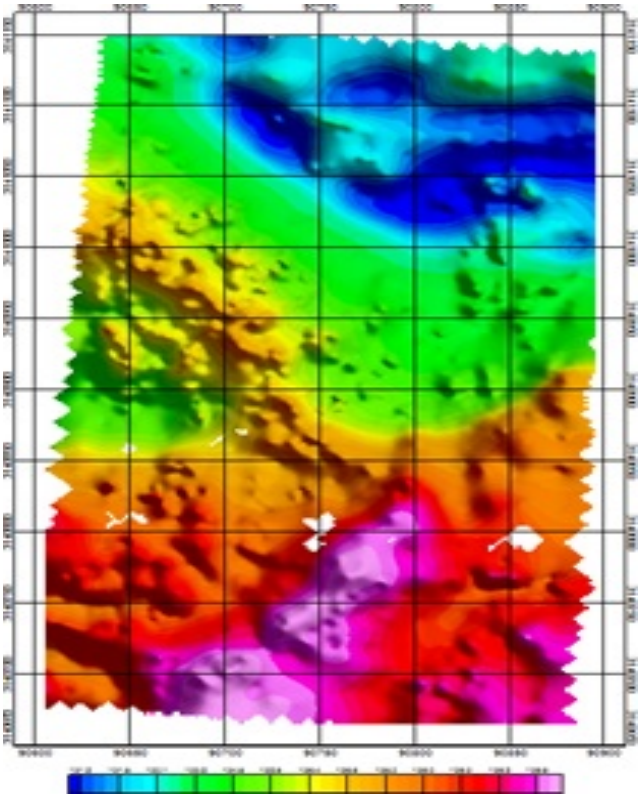

Fig. 5: The topographic image of the survey area.

2. GPR Data

The GPR data were acquired using the GSSI SIR2000 connected to the 400 MHz antenna to provide an optimum compromise between the required depth of penetration and resolution. The survey was conducted over 18 measuring cells ranging between D_{-1}, D_5, G_5, and G_{-1} (Fig. 4). Parallel grid pattern survey system was carried out along 474 profiles in the zig-zag pattern in S-N direction (Fig.6) to outline the subsurface tombs and archaeological features that may be present in the study area.

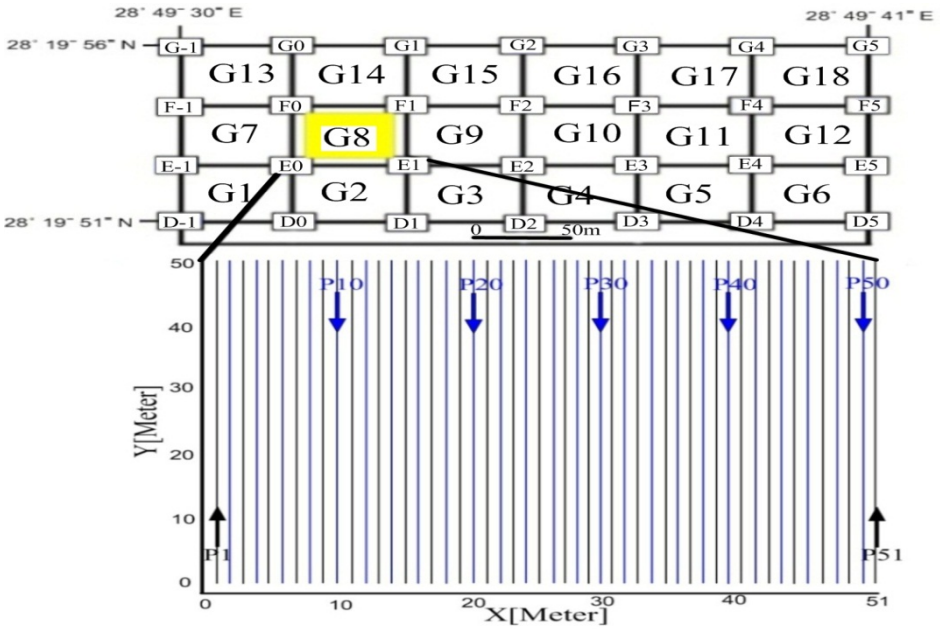

Fig. 6: The GPR surveyed grids in the study area.

Data Processing

Different types of noise are inherently present in GPR data. They include electronic background noise, mostly due to the equipment itself and modern electromagnetic interferences such as those generated from mobile phones, radio and television airwaves (Conyers, 2004). Raw data may also contain extraneous reflections such as above ground reflections, multiple subsurface reflections, and point source hyperbolae making the results difficult to interpret (Conyers, 2004). Once raw data has been cleaned and enhanced, a number of analytical and transformation processes may be applied to extract velocity information and make profiles easier to interpret. The complete GPR data set has been analyzed using Reflexw software Version 7.0 (Sandmeier, 2009). Processing steps include: (1) background removing filter remove the horizontal banding that appears in many GPR records due to the "ringing" of some antennas, horizontal bands are recorded in most profiles (Shih and Doolittle 1984; Sternberg and McGill, 1995). These bands can be obscure reflection data that would be visible on some profiles, (2) band Pass Filter this filter is specified by the setting of four frequency values. The first point

determines the low-cut frequency values. The second point is the beginning of the plateau (lower plateau). Between the low-cut frequency and the beginning of the plateau the filter is represented by a cosine-window respectively. The third point determines the end of the plateau (upper plateau) and the fourth the high cut frequency. The frequency spectrum below the low cut and above the high cut frequency is set to zero. Values are used here (200, 250, 500 and 550), (3) running average acts on the chosen number of traces. The filter performs running average over a chosen number of traces for each time step. The filter method suppresses trace dependent noise. Its effect is to emphasize horizontally coherent energy, (4) energy decay filter is used. The medium decay curve is specified from the present traces. When the filter is applied on this curve, each data point of each trace is divided by the decay curve values. When the energy decay curve is multiplied, all data points are multiplied by a scaling factor. The value of the scaling used here is "1", (5) trace interpol-3D file this processing steps adjusts the length and the number of traces for each radar profile.

There are two parameters; trace increment and profile length. The value of trace increment applied on the sections is 0.09 and the profile length is 50 m and (6) x flip profiles this processing step can overturn the radar profile in x-direction. This processing step is applied when the survey is applied by using zig-zag pattern. It is useful in following the expected features at successive radar profiles.

When the travel times of the radar pulses are measured, and their intra-ground velocity known, then distance or depth of the ground can be accurately to eventually render a 3D data set (Conyers and Lucius, 1996). The propagation velocity of the radar waves was estimated using the relative dielectric permittivity (RDP) of this area which is represented by hard limestone.

$\sqrt{RDP} = \frac{C}{V}$ (1) Where c is the velocity of light (0.298 m/ns) and v is the velocity of radar waves. According to Eq. (1), the velocity calculated is m/ns.

Also we used the velocity value of the radar wave from the previous study in study area in the same season. The calculated velocity was consistent to that used in previous study and has been used in time/depth conversion. Velocity (V) = Distance (m) / One way time (ns) = 1/ 6.5 = 0.15 m/ns (Diaa, 2015). The velocity of the materials which found in the study area =15m/ns according to (Annan, 2003).

Data Interpretation

GPR data interpretation is an important step to determine the size, shape, depth, and location of the anomalies that appears on the processed sections and discriminate them from the other undesired reflections. It also involves tracing the anomalies that appear on the successive sections to determine the subsurface extend and the expected depth of the buried objects that found in the surveyed grids. The results are displayed in two categories: two dimension cross section (2D) and three dimension (time slicing and 3D cube).

Study area divided into 18 grids and GPR data collected and applied the same processing steps on every grid separately after that we found all grids except grid no.8 does not have any important archaeological features and most profiles shows a flat layer, ferruginous Sandston bands and some bedding strata.

Time Slice Maps

Time slicing is a technique for constructing plan view maps of an area with specific depth ranges isolated. This not only makes interpretation of the data in the horizontal plane, but also allows the user to isolate specific depths for examination, or properly, the two way travel time of reflected waves. Time slice technique made the GPR method one of the most precise tools for mapping buried features (Conyers, 2006). Time slices are recently popular in archaeological and historical investigations (Leckebusch et al., 2003; Leucci and Negri, 2006; Leckebusch et al., 2008; Yalciner et al., 2009).

Now GPR users commonly use 3D mapping and computer generated visualization programs to study much larger areas of the subsurface (Conyers, 2013). These new standard visualization techniques produce amplitude slice maps from 2D reflection profiles (Linford, 2014) and recently from 3D data collected using multi antenna arrays that generate "real" 3D output (Conyers and Leckebusch 2010; Novo et al. 2008; Trinks et al., 2010). For small zones a more complete understanding of the subsurface can be achieved by means of various 3D data presentations, including 3D cubes, chair views and slices parallel to the axes or along arbitrary directions.

Several literatures (Milligan and Atkin, 1992; Goodman and Nishimura, 1993; Goodman et al., 1994) have presented the results of time slicing at various archaeological sites, and some conference paper (Nishimura and Kamei, 1990; Annan et al.,1992; Olhoeft, 1994) indicate that radar time slices and 3D image rendering of GPR data sets are beginning to be practiced . None the less, the use of time slicing has still yet to become a widely practiced and regular data analysis technique by the GPR user. Viewing amplitude changes in a series of horizontal time slices within the ground is analogous to studying geological and archaeological changes in equal time depth layers (Arnold et al., 1997; Goodman et al., 1995; Malagodi et al., 1996).

The ability to map this site in three dimensions using amplitude slice maps allows an interpretation of a scenario for the construction, abandonment, burial archaeological structures. The time slice analysis of GPR data has been accelerated by the requirements for making useful data presentations for archaeologists. The complexity of stratigraphic interfaces in the ground and changes in topography and surface materials can produce amplitude "anomalies" in the ground that are a function of the way data are resampled during processing.

The burial features may appear as either low amplitude or high amplitude reflections in slices, and truncations or breaks in stratigraphy in profiles (Conyers, 2004 and 2006). Columns and walls seen in profiles as vertically stacked reflections topped with hyperbola (Abbas et al., 2005; Barone et al., 2011; Conyers, 2004; Bonomo et al., 2010; Nuzzoet et al., 2009; Yalcineret et al., 2009). In time slicing maps walls of the conestruction will be imaged or appearerd as linear reflection which, can be used to define structures extents (Kavamme, 2008; Ruffell et al., 2009). Walls and columns generally produce high amplitude reflection due to constrasting velocities between walls and surroundign materials (Conyers, 2004 and 2009).

Time Slice Creation

Radar profiles in grid no. 8 were collected in a Zig-zag pattern across the survey grids at each of Grids. 1 m profile interval was believed to be sufficient to map the desired targets. Time slice made in consecutive and time interval was 5 ns. To create useful time slices, the time averaged and spatially averaged amplitudes are were gridded using information from surrounding points. The resulting gridded data were used to create time slice maps.

Application of Time Slice

Time slices were generated every 5 ns (approximately 37 cm depth). Building of time slices requires defining the upper limit (binning) and the lower limit (ending) of time slices. We put 5 ns approximately 37 cm depth the upper limit and 50 ns approximately 3.75 cm depth the lower limit (Fig. 7 and 8) because of the expected archaeological features which appeared in profiles no. 2, 3, 4, 13, 14, 15, 22, 23, 24, 35, 36, 37 and 38 located between 5ns and nearly 40 ns. We generated 10 time slices.

Results of Time Slice

An analysis of the spatial distribution of the amplitudes, in the form of amplitude time-slices (Conyers and Goodman, 1997) can often produce high-resolution maps of the subsurface. If amplitude changes can be related to the presence or absence of important buried features and stratigraphy, the location of higher or lower amplitudes at specific depths can be used to reconstruct the subsurface in 3D (Conyers et al., 2002). Thus, a number of radar signal amplitude time slices were constructed from the GPR records of grid 8.

Ten times slices representations, using the same time interval. It is clear to notice the important structures, which represent in high or low amplitude anomalies that reveal the extension of the important archaeological features, which may be the tombs and walls of buried tombs.

In (Fig. 7 and 8) there are high amplitude zone (A1) locates in northeast part at 5ns this zone about 12 m×15 m marked by blue circle. Anomaly A1 appear at 5ns about 0. 37 m depth, 10ns, 15ns, 20ns, 25ns, 30ns, 35ns and ended at 40 ns about 3 m depth. At 30 ns -40 ns, Anomaly A1decrease because of the attenuation of radar wave, which reflect the ending of the expected archaeological features.

Low amplitude zone (A2) locates in central east part at 5ns this zone about 8 m×10 m marked by blue circle. Anomaly A2 appear at 5ns about 0. 37 m depth, 10ns and 25ns. Anomaly A2 disappears at 15ns and 20ns then appears second time at 25ns about 1.78m depth and disappears at 30 ns, 35na and 40 ns. Appearing and disappearing of anomaly may be because of tombs are founding at at different burial levels.

High amplitude zone (A3) locates in central southeast part at 5ns this zone about 8 m×7 m marked by blue circle. Anomaly A3 appear at 5ns about 0. 37 m depth, 10ns, 15ns, 20ns, 25ns, 30ns, 35ns and ended at 40 ns about 3 m depth.

Anomaly A3 appears at 15ns, 20ns and 25ns about 12 m×10 m marked by blue circle Anomaly A3 decrease because of the attenuation of radar wave, which reflect the ending of the expected archaeological features.

High amplitude zone (A4) locates in central northeast part at 20ns this zone about 6 m×10 m marked by blue circle. Anomaly A4 appears at 20ns and disappears at 5ns, 10ns, 15ns, 25ns, 30ns, 35ns, 40ns, 45ns and 50ns. Disappearing of anomaly may be because the tombs are found at different burial levels. Die out of anomaly at time slices 45 and 50 ns reveals the ending of the expected archaeological features.

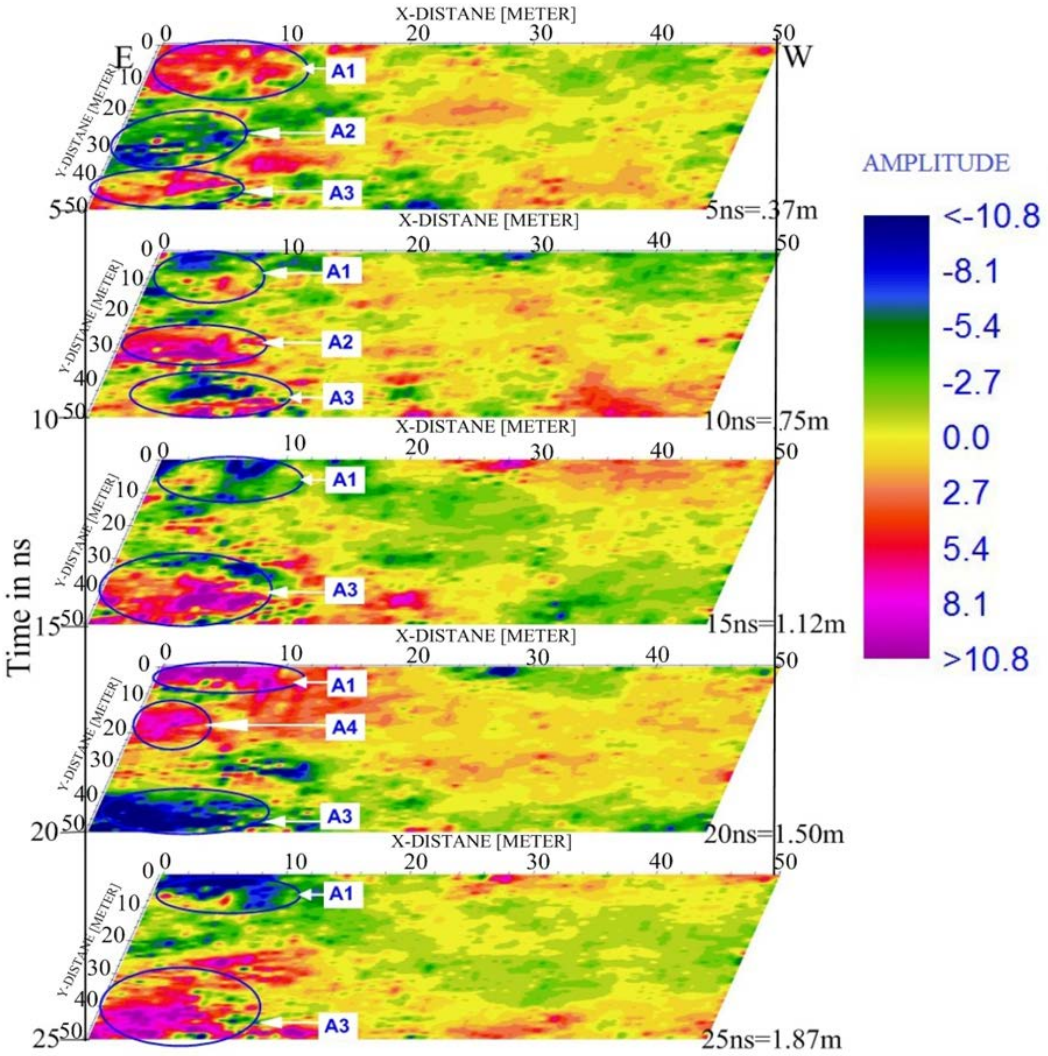

Fig. 7: shows time slice from 5ns-25ns

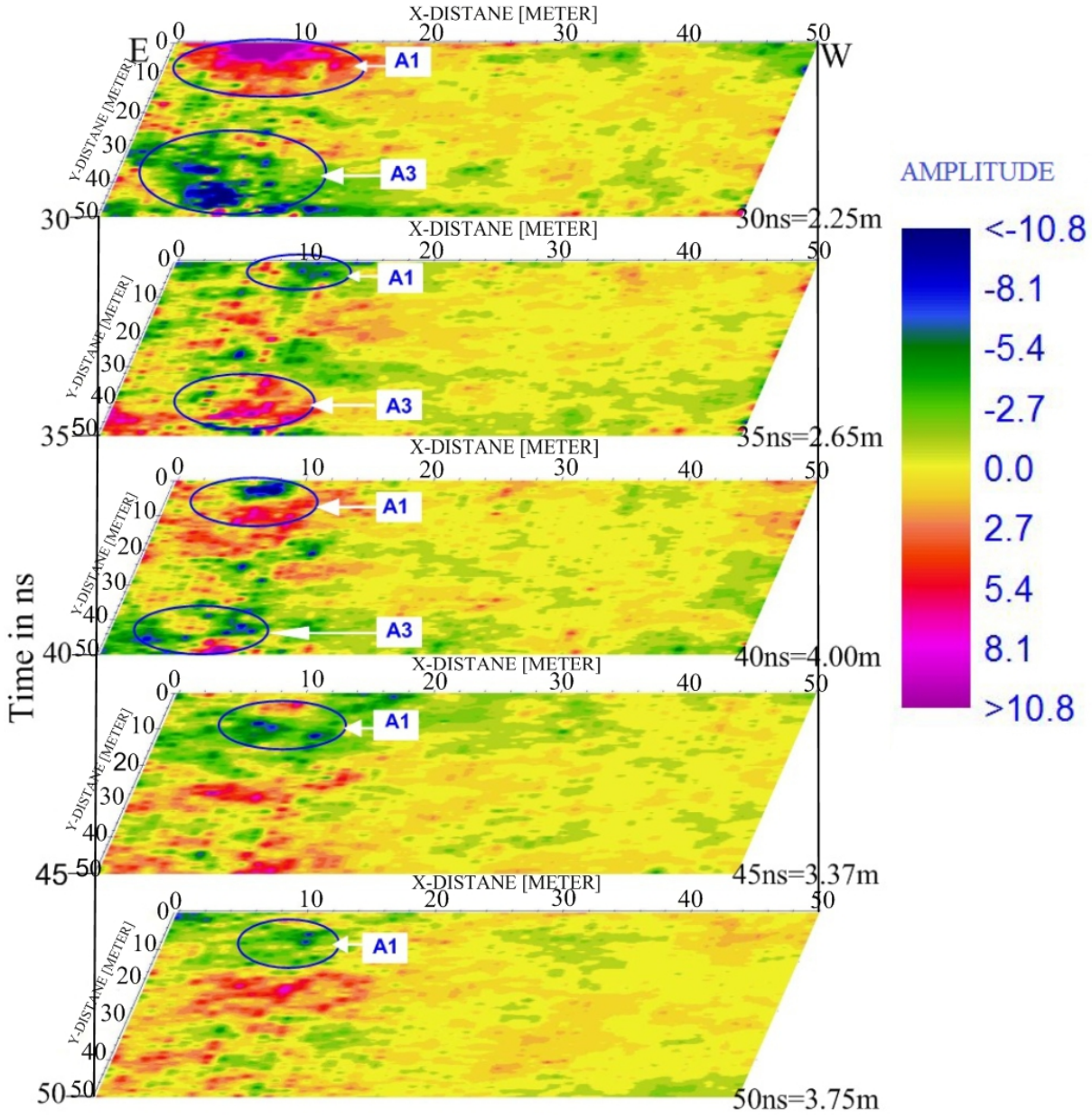

Fig. 8: shows time slice from 30ns-50ns

2D profiles

There are four objects are repeated in 2D GPR profiles in grid no.8.

Object number One

The object no. 1 appear in the radar profiles no. P2, P3 and P4 this feature marked by blue circles at horizontal distance between 19-29m, 28-38m and 26-33m respectively and vertical depth between 1- 2 m (Fig.8).

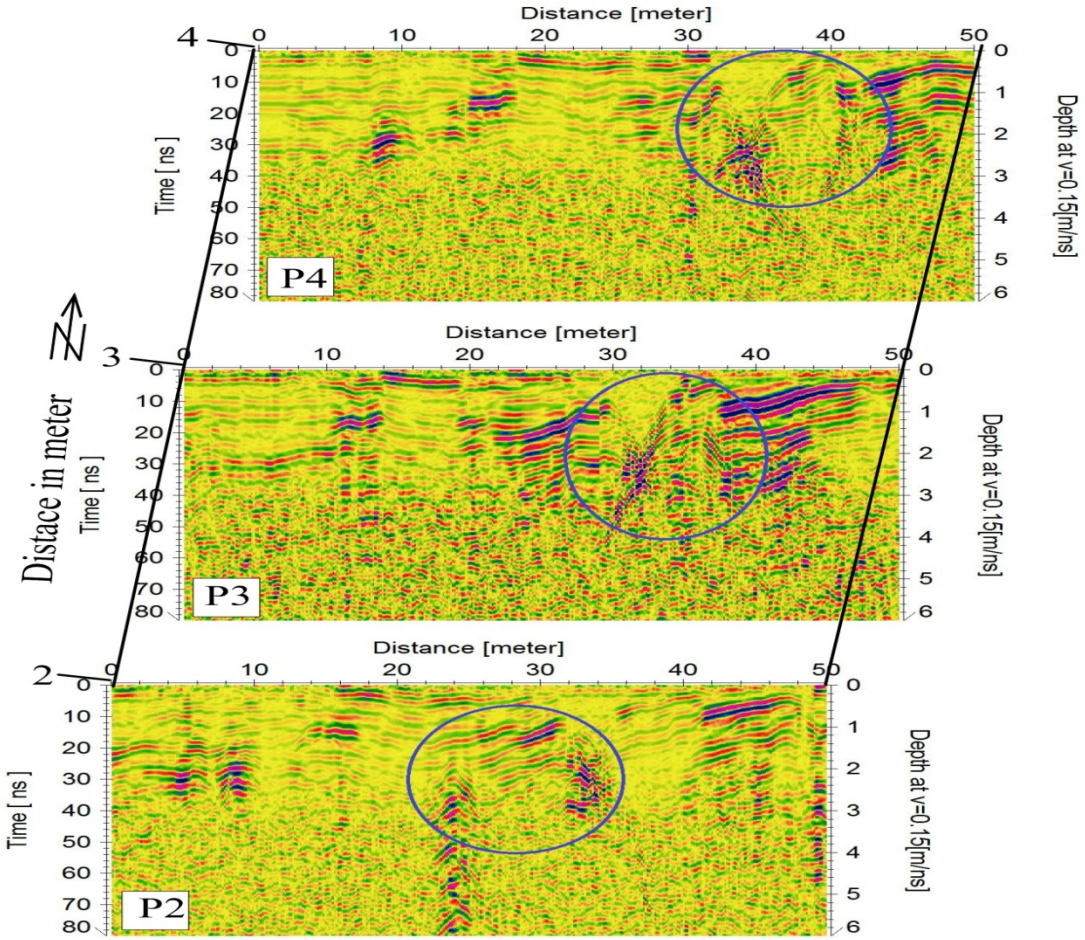

Fig. 8: Object no. one appears in profiles 2, 3 and 4 marked by blue circles.

Object number Two

The object no. 2 appear in the radar profiles no.22, 23 and 24 another feature marked by blue circles appears at horizontal distance between 9-12, 13-16 and 9-12 m respectively at depth of 1 m (Fig.9).

IJISET - International Journal of Innovative Science, Engineering & Technology, Vol. 4 Issue 2, February 2017
ISSN (Online) 2348 – 7968 | Impact Factor (2016) – 5.264
www.ijiset.com

Object number Three

The object no. 3 appear in the radar profiles no**.** 35, 36, 37and 38 another feature marked by blue circles appears at horizontal distance between 25-35, 29-36, 43-50 and 45-50 m respectively at depth of 40 cm (Fig.10)

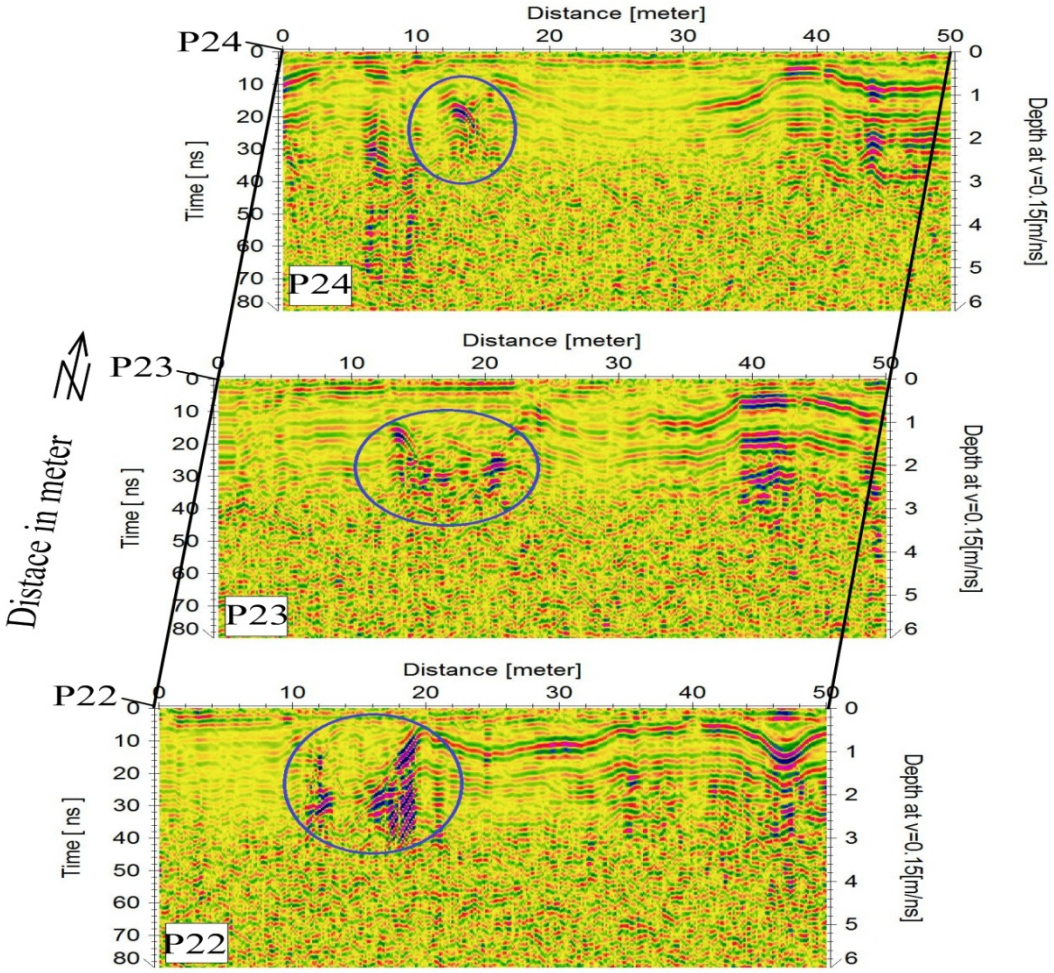

Fig. 9: shows object no. 2 appears in profiles 22, 23 and 24 marked by blue circles.

IJISET - International Journal of Innovative Science, Engineering & Technology, Vol. 4 Issue 2, February 2017
ISSN (Online) 2348 – 7968 | Impact Factor (2016) – 5.264
www.ijiset.com

Object number Four

The object no. 4 appear in the radar profiles no.13, 14 and 15 marked by blue circles at horizontal distance between 21-25, 21-25 and 23-25m at depth of 20cm-2.60 m (Fig.11).

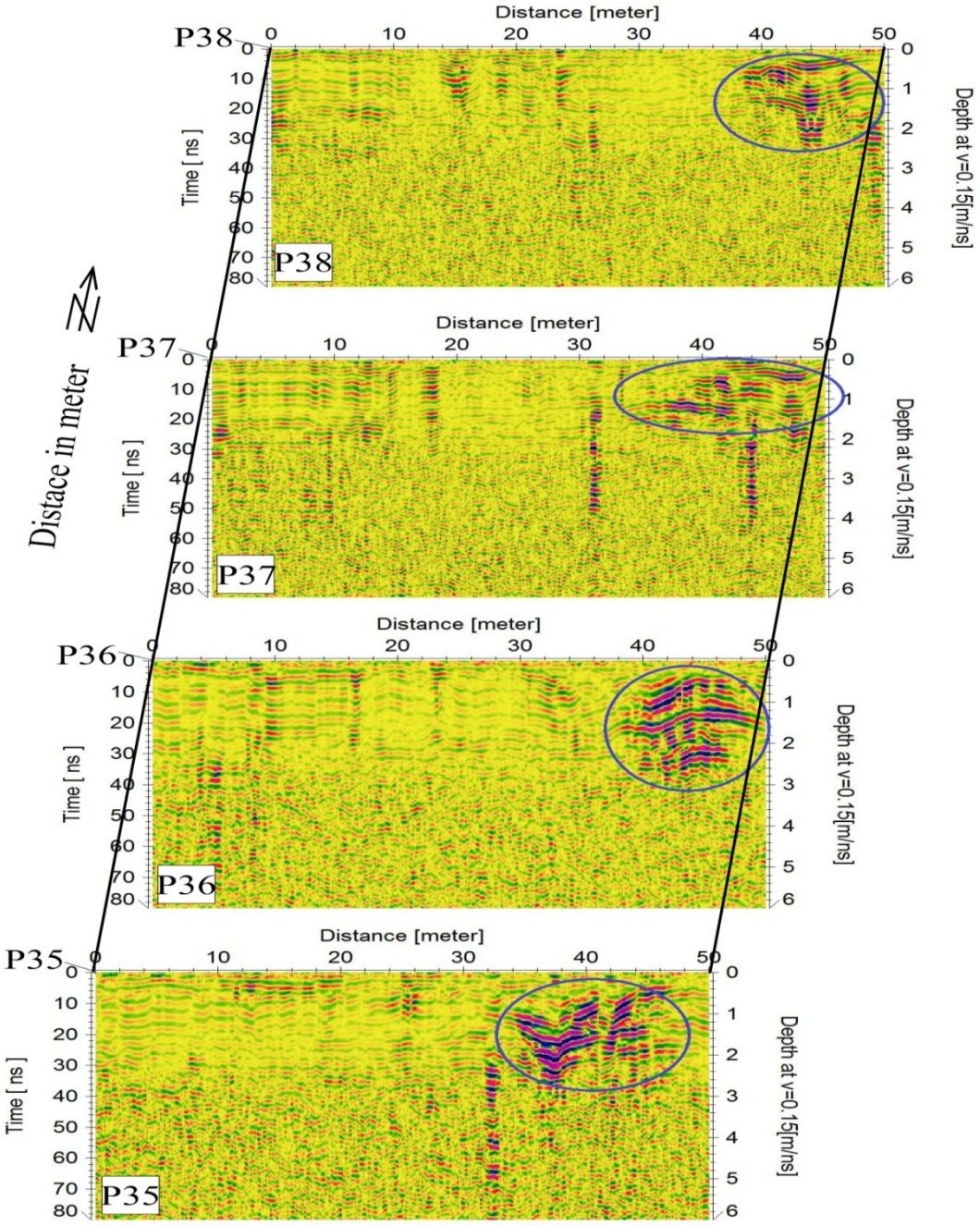

Fig. 10: shows object no. 3 appears in profiles 35, 36, 37and 38 marked by blue circles.

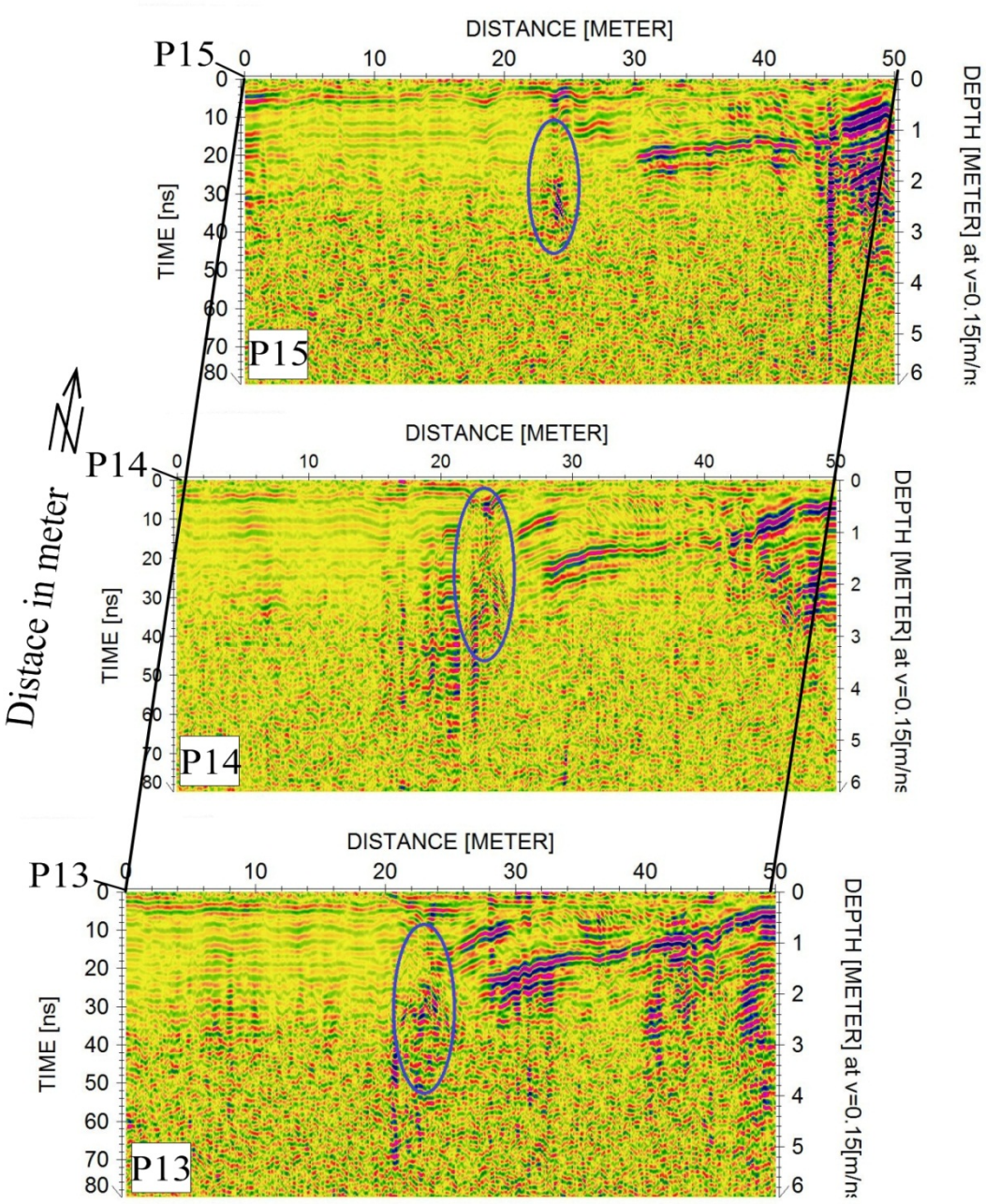

Fig. 11: shows object no. 4 appears in profiles 13, 14 and 15 marked by blue circles.

3D Cube

There is increasing use of 3-D surveys, where closely spaced lines give sufficiently dense data coverage for the construction of 3-D block models (Beres et al 1995). The data can be processed and exported into a 3-D visualization. The 3-D cube interpreted data in more detail than was possible based on widely

spaced 2-D profiles. 3D visualization is used to view and analyses the depth and geometry of the archaeological features.

3D views give clearer image of the subsurface over the survey area where the distributions of anomalies are well mapped. 3-D displays and time slices are used to show the relative locations of buried utilities. The processed GPR profiles can be represented in 3D cube by using Reflexw program.

3D Cube Generation

Reflexw program allows to import and to analyses automatically rectangular 3D GPR data which have been acquired along 2D-parallel lines in one or two perpendicular directions. The 3D data can also be displayed within a 3D cube. 3D visualization includes chair cuts, slices and variable capacity. Figure no. 12 shows (A) 3D cube and (B) object no. 1 which appears in profiles 2, 3, and 4 in 3D intersects. The important anomaly marked by blue circle.

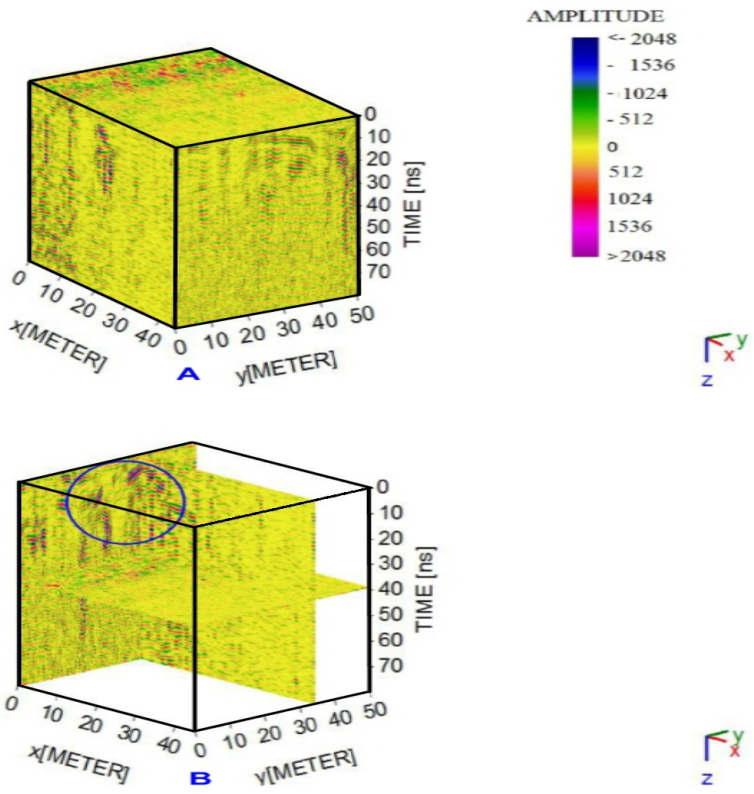

Fig.12: shows (A) 3D Cube and (B) object no.1 in 3D intersect.

Figure no. 13 show no. of objects marked by blue circles. (A) Shows the object no. two which represents the important anomaly that appears in profiles no.13, 14, and 15 in 3D intersects. (B) Shows the object no. 3 which represents the important anomaly that appears in profiles no. 22, 23, and 24 in 3D intersects. (C) Shows the object no. 4 which represents important anomaly that appears in profiles no. 35, 36, 37, and 38 in 3D intersects.

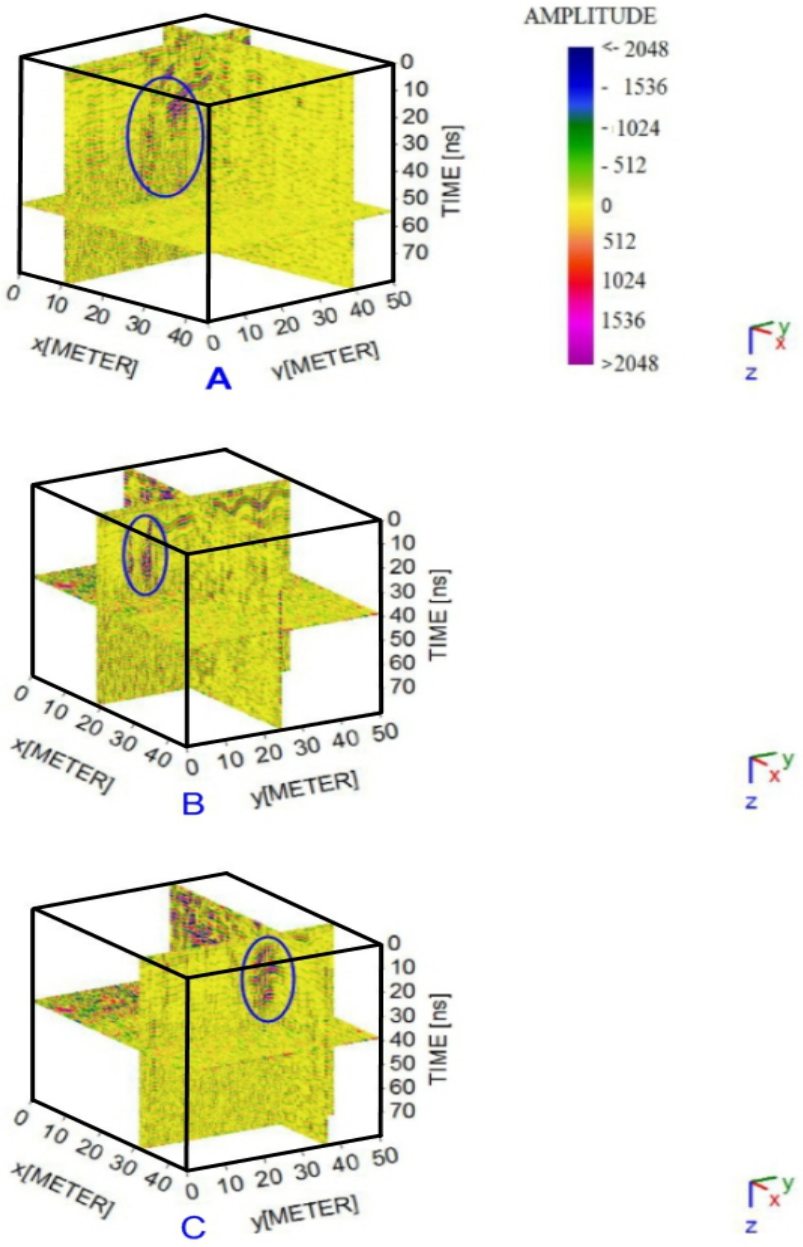

Fig.13: (A) objects no. 2, (B) 3 and (C) 4 in 3D intersect.

Conclusion

The results of GPR survey in the study area reveal the presence of four expected archaeological features. The object no 1 repeated in profiles no. 2, 3, and 4 beside that, object no. 3 repeated in profiles no. 35, 36, 37, and 38. Both objects may be are archaeological features like tombs. In addition to objects no. 2 and 4 appeared in profiles no.22, 23, 24 and 13, 14, 15 respectively these two objects may be tunnels or corridors. Depth of objects between 33cm-3.75m

Acknowledgements

I would like to thank my Supervisors for their suggestions and comments. I greatly appreciate the staff members of the Geoelectric Lab., NRIAG, Egypt, for their help in data acquisition.

References

Abbas A. M., Tareq F., Fathy A. S., Ahmed S. and Mancheol Suh, 2005b. Archaeological Investigation of the Eastern Extensions of theKarnak Temple Using Ground Penetrating Radar and Magnetic Tools. Geoarchaeology 20(5):537-554.

Annan, A. P., 2003. Ground Penetrating Radar: Principles, Procedures and Applications, pp.47.

Annan, A. P., Brewster, M. L., Greenhouse, J. P., Regman, J. D., 1992. Geophysical monitoring of DNAPL migration in sandy aquifer. Abestact, technical program, Socity of Exploration Geophysists Annual International Meeting, New Orleans, 25-29 October, 344-347.

Arnold, J. E., E. L. Ambos, and D. O. Larson, 1997. Geophysical Surveys of Stratigaphicaaly Complex Island California Sites: New Implications for Household Archaeology Antiquity 71:157-168.

Barone, P. M., T. Bellomo, E. Mattei, S. E. Lauro, and E. Pettinelli, 2011. Ground penetrating Radar in the Regio III (Pompeii, Italy): Archaeological Evidence. Archaeological Prospection 18:187-194.

Beres, M., Green, A., Huggenberger, P. and Horstmeyer H., 1995. Mapping the architecture of glacio fluvial sediments with 3D georadar. Geology,23, 1087-1090.

Bonomo, Néstor, Ana Osella, and Norma Ratto, 2010. Detecting and mapping buried buildings with Ground Penetrating Radar at an ancient village in northwestern Argentina. Journal of Archaeological Science. 37:3247-3255.

Conyers, L. B., 2004. Ground Penetrating Radar for Archaeology. Alta Mira Press, Lanham.

Conyers, L. B., 2006. Ground penetrating radar techniques to discover and map historic graves. Historical Archaeology. 40, 3, 64-73.

Conyers, L. B., 2009. Ground Penetrating Radar for landscape archaeology: Method and applications. In Seeing the Unseen, edited by Stefano Campana and Salvatore Piro, pp. 245-255.

Conyers L. B., 2013. Ground penetrating Radar for Archaeology, 3rd edn. Rowman and Littlefield Publishers, Alta Mira Press, Latham, Maryland.

Conyers L. B. and Leckebusch J., 2010. Geophysical archaeology research agendas for the future: Some ground penetrating radar examples. Archaeological Prospection 17, 117–123.

Conyers, L. B., E. G. Ernenwein, and L.-A. Bedal, 2002. Ground Penetrating Radar Discovery at Petra, Jordan. Antiquity 76:339–340.

Conyers, L. B. and Goodman, D., 1997. Ground Penetrating Radar: An introduction for Archaeologists. Altamira Press, Walnut Creek, California 0-7619-89 27-7. 232 pages, 58 figures, 8 plates.

Conyers L. B. and Lucius, J.E., 1996. Velocity analysis in archaeological ground-penetrating radar studies. Archaeological Prospection 3, 312– 333.

Davis, J. L. and Annan A. P., 1989. Ground penetrating radar for high resolution mapping of soil and rock stratigraphy. Geophys. Prospect., Vol. 37.

Diaa H., 2015. Archaeo Geophysical Investigation for the Greco Roman Necropolis at Kilo 6 of the Golden Mummies Valley, Bahariya Oasis, Egypt. :M. Sc Thesis, Mansoura University.

Fischer, P. M., S. G. W. Follin, and P. Ulriksen 1980. Subsurface Interface Radar Survey at Hala Sultan Tekke, Cyprus. In Applications of Technical Devices in Archaeology, edited by Peter M. Fischer. Studies in Mediterranean Archaeology 63:48–51.

Goodman, D., and Y. Nishimura 1993. A Ground Radar View of Japanese Burial Mounds. Antiquity 67:349–354.

Goodman, D., 1994. Ground Penetrating Radar Simulation in Engineering and Archaeology. Geophysics 50(2): 224–232.

Goodman D., Y. Nishimura, and J. D. Rogers, 1995. GPR Time Slices in Archaeological Prospection. Archaeological Prospection 2 (2):85–89.

Goodman, D., Y. Nishimura, H. Hongo, and O. Maasaki, 1998. GPR Amplitude Rendering in Archaeology. In Proceedings of the Seventh International Conference on Ground Penetrating Radar, pp. 91–92.

Goodman, D., Y. Nishimura, T. Uno, and T. Yamamoto1994.Ground penetrating Radar Survey of Medieval Kiln Sites in SuzuCity, Western Japan. Archaeometry 36(2):317-326.

Imai, T., T. Sakayama, and T. Kanemori, 1987. Use of GPR and Resistivity Surveys for Archaeological Investigations. Geophysics 52:137–150.

Khozym A. S., 2003. Geophysical Archaeoprospection in Some Archaeological Sites at El Baharya Oasis, Giza, Egypt :Ph. D., Thesis Ain Shams University. Cairo.

Khozym A. S., 2007. Geophysical Prospection in some Archaeological sites in Saqqara area, Giza, Egypt :Msc., Thesis Ain Shams University. Cairo.

Kvamme Kenneth L., 2008. Archaeological Prospecting at the Double Ditch State Historic Site, North Dakota, USA. Archaeological Prospection 15:62-79.

Leckebusch, Jürg, 2003. Ground penetrating Radar:A ModernThree dimensional Prospection Method. Archaeological Prospection10,213-240.

Leckebusch J., Weibel A. and Bühler F., 2008. Semi-automatic feature extraction from GPR data. Near Surface Geophysics. 6, 2, 75-84.

Leucci G., Negri S., 2006. Use of ground penetrating radar to map subsurface archaeological features in an urban area. Journal of Archaeological Science. 33, 502-512.

Linford N., 2014. Rapid processing of GPR time slices for data visualisation during field acquisition. In: Proceedings of the 15th International Conference on Ground Penetrating Radar, pp. 731–735.

Magdy A. Atya, FathyA. S., Abbas, A. M. and Mahfooz H., 2008. Ground penetrating radar exploration for ancient monuments at the Valley of Mummies

-Kilo 6, Bahariya Oasis, Egypt, Journal of Applied Geophysices (2008), doi:10.1016/ j.jappgeo. 20 08.11.0 09.

Magdy A. Atya, Fathy A. S., Abbas A. M. and Mahfooz H., 2012. GPR investigation to the archaeological remains in Mut temple, Luxor, Upper Egypt,NRIAG Journal of Astronomy and Geophysices (2012),doi:10.1016/ j.nriag. 20 12.11.0 02.

Mahfooz H., Magdy A. Atya, Azza M. Hassan, Motoyuki Sato,Thomas Wonik, and Abeer A. El-Kenawy, 2008. Shallow geophysical investigations at the Akhmim archaeological site, Suhag, Egypt, 5, pp.136-143.

Malagodi, S., L. Orlando, and S. Piro 1996. Approaches to increase resolution of radar signal. In Proceedings of the Sixth International Conference on Ground Penetrating Radar: 283–288.

Milligan R., and Atkin, M., 1992. The use of ground Penetrating Radar within a digital environment on archaeological sites, in computer applications and quantitatinve methods in archaeology.21-32.

Nishimura Y., and Kamei H., 1990. Proceeding of the 27th International Conference on Archaeology, Heidelberg.

Novo A., Grasmueck M., Viggiano D. A. and Lorenzo H., 2008. 3D GPR in archaeology: what can be gained from dense data acquisition and processing? In: Proceedings of the 12th International Conference on Ground Penetrating Radar (GPR 2008), Birmingham, pp. 16–19.

Nuzzoet, Luigia, Giovanni Leucci, and Sergio Negri, 2009. GPR, ERT and Magnetic Investigations Inside the Martyrium of St Philip, Hierapolis, Turkey. Archaeological Prospection 16:177-192.

Olhoeft, G. R., 1994. Proceeding of the 5th International Conference on Ground Penetrating Radar, Kithener, Ontario (Waterloo Center for Groundwater Research):133-144.

Ruffell, Alastai, Alan McCabe, Colm Donnelly, and Brian Sloan, 2009. Location and Assessment of an Historic (150-160 Years Old) Mass Grave Using Geographic and Ground Penetrating Radar Investigation, NW Ireland. Journal of Forensic Sciences 54(2):382-394.

Sandmeier K. J., 2009. Reflexw Version 7.0 Sandmeier Scientific Software: Karlsruhe, Germany.

Sheets P. D., W. M. Loker, H. A. W. Spetzler, and R. W. Ware, 1985. Geophysical Exploration for Ancient Maya Housing at Ceren, El Salvador. National Geographic Research Reports 20:645–656.

Shih S. F., and J. A. Doolittle, 1984. Using radar to Investigate Organic Soil Thickness in the Florida Evergaldes. Soil Science Society of America Journal 48:651-656.

Sternberg B. K., and J. W. McGill, 1995. Archaeology Studies in Southern Arizona Using Ground Penetrating Radar .Journal of Applied Geophysics 33:209-225.

Sayed H., 2012.Ground Penetrating Radar (GPR) Investigations for Architectural Heritage Preservation:The Case of Habib Sakakini Palace, Cairo, Egypt,2, 189-197.

Trinks I., Johansson B., Gustafsson J., Milsson J., Friborg J. and Gustafsson J.N. et al., 2010. Efficient, large scale archaeological prospection using true three dimensional ground penetrating radar array system. Archaeological Prospection 17, 175–186.

Vickers, R. S., and L. T. Dolphin, 1975. A Communication on an Archaeological Radar Experiment at Chaco Canyon, New Mexico. MASCA Newsletter 11(1):6–8.

Yalciner C., Bano M., Kadıoglu M., Karabacak V., Meghraoui M. and Altunel E., 2009. New temple discovery at the archaeological site of Nysa (western turkey) using GPR method. Journal of Archaeological Science, 36, 8, 1680-1689.